PRELIMINARY UNCERTAINTY ASSESSMENT OF THE CONTAINMENT BEHAVIOR FOR THE PHEBUS FPT1 TEST

Michela Angelucci, Sandro Paci
University of Pisa, Italy

ABSTRACT

In recent years, an ever-growing attention has been paid to the assessment of the uncertainties linked to simulation results from computer codes employed in the safety analysis of Nuclear Power Plants (NPPs). These codes have been improved over the years, and they have reached a high level of maturity with regards to their ability to simulate complex systems and scenarios. This is particularly important when it comes to Severe Accidents (SAs). However, a thorough quantification of the uncertainties related to SA codes predictions is still needed. In this framework, the present paper reports a preliminary Uncertainty And Sensitivity Analysis (UASA) of the containment behavior for the PHEBUS FPT1 test. The MELCOR 2.2 code has been employed to model the containment vessel of the PHEBUS facility, whereas the uncertainty investigation has been carried out through the propagation of a limited set of uncertain input parameters. The Wilks formula has been then used to calculate the minimum number of code runs (minimum sample size) necessary to achieve a 95%/95% confidence and probability levels. As for the outcomes, considering that the correct estimation of a possible radiological source term to the environment is of high relevance to the safety assessment of NPPs, the focus of the entire analysis has been placed on the mass of aerosol suspended in the containment atmosphere. The uncertainty band has been derived for the selected Figure of Merit (FOM), and an initial search for the parameters with the highest influence on the response has been conducted. Results show that the uncertainty band varies in time along with the scenario unfolding, and it presents a wide broadening concurrently with the reaching of the peak of aerosol in the containment atmosphere.

Keywords: Uncertainty Quantification, Severe Accidents, Sensitivity Analysis, MELCOR, MUSA.

INTRODUCTION

In the framework of the international PHEBUS research program [1], five in-pile integral experiments were conducted in Cadarache (France) between 1993 and 2004, with the main focus on core degradation and consequent Fission Products (FPs) release (and transport) during a Severe Accident (SA) sequence. The entire campaign was conducted in the PHEBUS facility, the in-depth description of which is reported in [2]–[4]. The facility was designed as a representative of a Pressurized Water Reactor (PWR) under core-melt accidental conditions. More specifically, a typical French 900 MWe PWR was reproduced in a 1:5000 scale, with the cold leg entering at the center of the containment vessel to simulate a cold leg loss of coolant accident.

Several tests were performed, investigating different fuel burn-up levels, control rod materials, and thermal-hydraulic conditions. In particular, for the PHEBUS Fission Product Test 1 (FPT1), a 1 m long PWR fuel bundle with an overall burnup of 23.4 GWd/tU was considered. The bundle was composed of 18 rods, 2 instrumented fresh fuel rods and a Ag-In-Cd control rod, and its degradation was studied under a highly oxidizing atmosphere. As a result, a certain amount of data related to FPs release, transport and chemical behavior was obtained [4].

In the last decades, the PHEBUS FPT1 has been extensively studied, and its data has been thoroughly employed to assess source-term evaluation models and to validate safety codes' results [5]–[10]. Several analyses, carried out with both integral and Computational Fluid Dynamic (CFD) codes, have been proposed, covering a broad range of aspects: from primary core degradation mechanisms to transport and deposition in the circuit, from material release to containment behavior, from thermal-hydraulics to source term [11]–[17].

More recently, the same PHEBUS FPT1 scenarios has been the subject of the training exercise performed within the "Management and Uncertainty of Severe Accidents" (MUSA) EURATOM project, the main aim of which is to foster the application of Best Estimate Plus Uncertainty (BEPU) methodologies to SAs [18]. In this framework, the simplified but still representative SA scenario that is the PHEBUS FPT1 has been employed to test Uncertainty Quantification (UQ) techniques, in the attempt to assess the uncertainties linked to SA codes' results [19]–[23].

In [21], an initial evaluation of the uncertainties linked to the results obtained using the MELCOR 2.2.18019 code ([24], [25]) is reported. The entire facility is modeled, and the first two phases (namely, degradation and aerosol phases) of the PHEBUS FPT1 scenario are simulated, with a focus on the "amount of aerosol in the containment atmosphere".

Complementary to this study, the present paper reports a preliminary Uncertainty And Sensitivity Analysis (UASA) of the containment behavior for the PHEBUS FPT1, through a standalone analysis of the containment itself. The uncertainty investigation, carried out through a series of MATLAB [26] scripts, is based on the propagation of the same limited set of input parameters, with the Wilks formula ([27], [28]) used to calculate the minimum number of runs necessary to achieve a 95%/95% confidence and probability levels. As for the outcomes, considering that the correct estimation of a possible radiological source term to the environment is of high relevance to the safety assessment of NPPs, the focus of the entire analysis is placed, once again, on the "mass of aerosol suspended in the containment atmosphere".

PHEBUS FPT1 CONTAINMENT MODEL

The MELCOR model for the PHEBUS containment, better described in [29], [30], is briefly summarized in this section. Considering the lumped-parameter nature of the MELCOR code, the characterization of the spatial domain is obtained using Control Volumes (CVs), connected through Flow Paths (FPs). The containment vessel walls and the three internal condensers are, instead, modeled by means of Heat Structures (HSs).

As it can be seen in Figure 1, 21 CVs are employed to simulate the containment vessel. More precisely, the sump is modeled by a single volume, whilst the remaining 20 CVs are devoted to the main cylindrical part of the containment, that is subdivided into three radial rings. Temperature and pressure are imposed as initial conditions for each CV, and their values are set as in [4], [31]. The different CVs are connected by means of 32 FPs.

For what concerns the walls, 15 HSs simulate the sump outer wall (WSU), the semi-elliptic bottom of the vessel (WB1, WB2), the semi-elliptic top of the vessel (W6T, W12T, W18T), the cylindrical outer wall (W13-W17), and the condensers (WET4, WET5, WET6, DRY). All the HSs (except the ones related to the condensers) are characterized by an imposed outer temperature evolving in time according to the test boundary conditions [4]. Inner temperatures are instead calculated, by the code itself, taking into account the heat exchange with the surrounding HSs. On the contrary, the HSs simulating the condensers have an imposed inner temperature evolving in time according to the test boundary conditions [4], whilst the outer temperature is calculated by the code. The characteristic length for each HS is imposed in a different way according to its orientation: the height of the wall is chosen for vertical cylindrical surfaces, whereas a value equal to the area of the wall divided by the perimeter is selected for horizontal surfaces, as suggested in [32]. As for the condensers, the characteristic length is set equal to the external diameter, so to have the correct condensation rate.

Finally, FPs and aerosol injections are placed inside the C1 volume in agreement with the real geometry of the system. Mass injection, Aerodynamic Mass Mean Diameter (AMMD) and source Geometrical Standard Deviation (GSD) are imposed, for different chemical elements, in accordance with [4].

Main dimensions of the containment vessel are reported in Table 1.

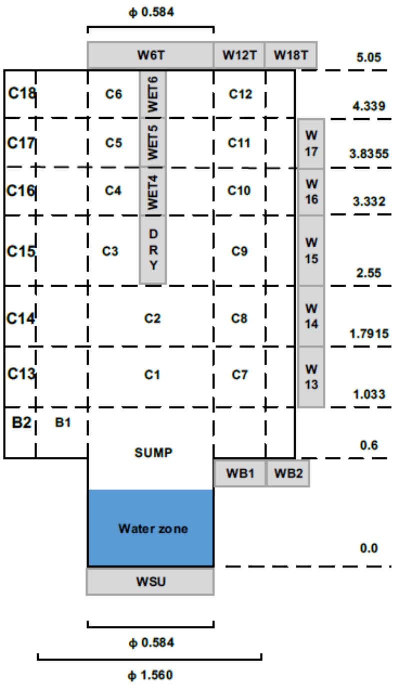

Figure 1: MELCOR nodalization.

	Dimension
Total volume	10 m^3
Total height	~ 5 m
Main diameter	1.8 m
Sump volume	0.1 m^3
Sump diameter	0.584 m
Water mass in the sump	105 kg
N. of condensers	3
Condensers "wet" surface	0.775 m^2
Condensers "dry" surface	0.336 m^2
Condensers "wet" length	1.718 m
Condensers "dry" length	0.782 m

Table 1: PHEBUS containment vessel main dimensions.

UASA STRATEGY

UNCERTAINTY METHODOLOGY

Several methodologies have been proposed and extensively used in thermal-hydraulics for the evaluation of uncertainties as a support of Best-Estimate (BE) safety analysis of NPPs [33], [34]. Among these, the GRS methodology [35] has been selected as starting point for the unfolding of the Uncertainty Analysis (UA) carried out in this work.

The chosen methodology is based on the propagation of the input parameters, together with a statistical evaluation of the code results. Input parameters and their distributions are user-selected, and samples are created by means of random sampling. The number of samples is chosen in accordance with the Wilks formula [36]: given proper probability α and confidence β levels for the UA, the minimum number of runs N is calculated, independently of the number of input parameters, using the following equations for one-sided (Eq. 1) and two-sided (Eq. 2) tolerance limits:

$$\beta = 1 - \alpha^N \qquad (1)$$

$$\beta = 1 - \alpha^N - (N-1)(1-\alpha)\alpha^{N-1} \qquad (2)$$

A total number of N runs are performed, starting from an initial BE case and varying simultaneously the input parameters accordingly to the created samples. The obtained results, in terms of the chosen output variable, are then analyzed on the basis of the selected tolerance limit: in the case of a one-sided tolerance limit, the maximum value corresponds to the α percentile with a β confidence level. In the case of a two-sided tolerance limit, instead, the minimum and maximum values can be evaluated together, and an uncertainty interval can be derived.
In the present work, a two-sided tolerance limit was selected, and a minimum of 93 runs was considered necessary to have a 95%/95% probability and confidence levels on the selected output variable, also called Figure Of Merit (FOM).

UNCERTAINTY CONFIGURATION

Taking into account the preliminary stage of the UA presented in this paper, a limited set of input parameters has been chosen. In addition, considering that the selected FOM for this analysis is the "mass of aerosol suspended in the containment atmosphere", the input parameters involved in the analysis are all related to aerosols' behavior and characterization. The list of the selected MELCOR input parameters is presented below:

- CHI: aerosol dynamic shape factor;
- GAMMA: aerosol agglomeration shape factor;
- FSLIP: particle slip coefficient;
- STICK: particle sticking coefficient;
- TURBDS turbulence dissipation rate;
- TKGOP: ration of the thermal conductivity of the gas over that of the particle;
- FTHERM: thermal accommodation coefficient;
- DELDIF: diffusion boundary layer thickness.

Reference values and distribution types are reported in Table 1. They have been set in accordance with [24], [37].

Parameter	*Reference Value*	*Distribution Type*	*Range of Variation*	
CHI	1.0	Beta	1.0	5.0
GAMMA	1.0	Beta	1.0	5.0
FSLIP	1.257	Beta	1.2	1.3
STICK	1.0	Beta	0.5	1.0
TURBDS	0.001	Uniform	0.00075	0.00125
TKGOP	0.005	Log-Uniform	0.006	0.06
FTHERM	2.25	Uniform	2.0	2.5
DELDIF	1.0e-5	Uniform	0.000005	0.0002

Table 1: Input parameters.

SENSITIVITY COEFFICIENTS

In order to gain an insight into the contribution of individual input parameters to the calculated uncertainty band, a sensitivity analysis has been performed. It is worth saying that it is not *a priori* sensitivity analysis, but rather it is based on the dataset obtained from the calculations launched for the UQ analysis.

As a first approach, the influence of input parameters on the selected FOM has been assessed using Correlation Coefficients (CCs) and their corresponding partial ones. In particular, Pearson and Spearman CCs have been employed as measures of linear and/or monotonic relationships among the input parameters and the FOM [38]. In both cases, the closer the coefficient is to ±1 the stronger is the correlation between the variable and the FOM. Pearson and Spearman CCs equations [39], [40] are reported in the following (Eq. 3 and Eq. 4, respectively):

$$\rho(x,y) = \frac{\sum_{i=1}^{n}(x_i - \bar{x})(y_i - \bar{y})}{\sqrt{\sum_{i=1}^{n}(x_i - \bar{x})^2 (y_i - \bar{y})^2}} \quad (3)$$

$$r_s(x,y) = 1 - \frac{6\sum_{i=1}^{n} d_i^2}{n(n^2 - 1)} \quad (4)$$

where $\bar{x}$ and $\bar{y}$ are means of variables x and y, n is the sample size, and d_i is the difference in ranks for x and y.

As for the partial CCs, they have been used with the aim of computing the correlation between each input parameter and the FOM, while taking into consideration the presence of other input parameters.

In addition, p-values have been calculated for each CC in order to test the statistical significance of the CC itself, as suggested in [38], [41]. In this regard, given a significance level (usually set as 0.05), the correlation is statistically significant if the p-value is smaller than the significance level. On the contrary, when the p-value is bigger than the significance level, the correlation is considered "not statistically significant".

RESULTS

As previously said, considering the safety relevance of a possible radiological source term to the environment, the focus of the entire analysis has been placed on one FOM, namely the "mass of aerosol suspended in the containment atmosphere". Given that the accuracy of the employed MELCOR model was demonstrated in [29], only results from the performed UASA will be reported hereafter. Both scalar and time-dependent analysis will be presented.

Outcomes from the 93 successful MELCOR 2.2 runs, necessary to achieve 95%/95% probability and confidence levels, have been collected in a dispersion plot as shown in **Error! Reference source not found.**.

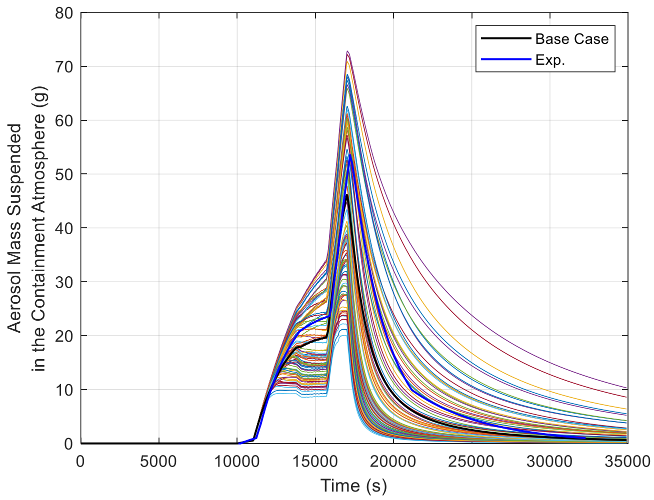

Figure 2: Dispersion plot for the FOM.

Few observations can be drawn from it:

- All the plotted results show a similar shape: in consistency with the evolution of the accidental scenario, an initial accumulation of aerosol in the containment atmosphere starts at around 11,000 s, with a slight delay with respect of the start of the pre-oxidation phase. It is then followed by a further rising in the mass of aerosol at around 16,000 s (correspondingly to the heat-up phase) leading to the peak at around 17,500 s;
- Notwithstanding the similarity in the timing evolution, differences can be observed when investigating the aerosol mass suspended in the containment atmosphere. The uncertainty band

varies in time along with the scenario unfolding, with a broadening in correspondence of the peak value. The uncertainty interval is then reduced;

- After the peak, all the curves show a steep decrease in the quantity of aerosol suspended in the containment atmosphere. However, the slopes of the curves differ, spanning over a broad range of values and leading to a certain degree of uncertainty in the aerosol quantity at the end of the calculation time. This behavior could most likely be explained by different velocities in the settling down of the aerosol particles present in the containment atmosphere, due to the predicted different effective diameters. Nonetheless, it should be noted that, for a simultaneous UQ analysis of both "mass of aerosol in the containment atmosphere" and "aerosol deposition in the containment", an additional study should be carried out increasing the number of runs as well as the sample size, employing the Wald formula for a multivariate approach [42], as suggested in [36].

An alternative way to present the obtained results is shown in **Error! Reference source not found.**, in which the Probability Density Function (PDF) for the peak value of the FOM is represented as both a discrete histogram plot and a continuous line. The empirical continuous PDF has been obtained by using the built-in MATLAB function "ksdensity" [43], in which normal kernels are employed to obtain a smoothed and continuous density estimation. As it can be seen, the output distribution is not symmetric, and it presents a shift toward mass values lower than 50 g. This indicates a tendency to underestimate the maximum value for the mass of aerosol in the containment atmosphere.

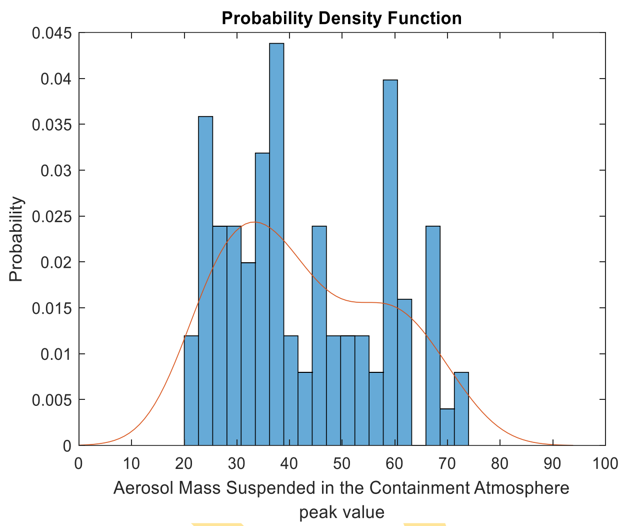

Figure 3: PDF – peak value of the FOM.

Considering the order statistics behind the Wilks formula, for each time step, the minimum and maximum values correspond to the 2.5th and 97.5th percentiles with a 95% confidence level. In particular, when considering the end of the calculation time, the extreme values obtained (reported in **Error! Reference source not found.**) denote an uncertainty interval of around 10 g. In the analysis of the peak value, instead, the uncertainty interval increases up to around 52 g (as it can be deducted from **Error! Reference source not found.**). These results provide some information about the level of uncertainty linked to the simulations' outcomes. However, it has to be point out that the calculated uncertainty interval has to be thought of in view of the used code (and its current development status), of the selected parameters' list, and to the BE model itself, which suffers from the so called user's effect.

	Value
max	10.31 g
min	0.075 g

Table 3: Extreme values- end of calculation time.

	Value
max	72.85 g
min	20.04 g

Table 4: Extreme values - peak.

Concerning the sensitivity analysis, the reason to perform it is twofold: to identify the input parameters with the highest influence on the addressed output response, and, in turn, to focus research on dominant parameters to effectively reduce the uncertainty linked to simulations.

As a first approach, four CCs have been considered for this analysis: Pearson, Partial Pearson, Spearman and Partial Spearman. However, no one of the selected input parameters seems to be predominant in the attempt to explain the uncertainty on the maximum value of the FOM. In fact, as it can be seen in **Error! Reference source not found.**, both Pearson and Partial Pearson CCs indicate that there is no significant linear relationship between the considered parameters and the FOM. In addition, p-values (shown in red in **Error! Reference source not found.**) have been calculated for both coefficients: values are greater than 0.05 (significance level), thus indicating that the correlation is "not statistically significant". The same assertions can be made for both Spearman and Partial Spearman CCs. **Error! Reference source not found.** shows that no one of the input parameters has a monotonic relationship with the FOM. Also in this case, calculated p-values (in black) do not contradict CCs results.

Additionally, Partial Pearson and Spearman coefficients have been calculated along the entire time interval considered in the calculations. For what concerns the former, even though it can be clearly seen (Figure 1) that Partial Pearson CC varies in time, its absolute value is always below 0.2, and no linear relationship can be claimed between any of the parameters and the chosen FOM. On the other side, analyzing results in **Error! Reference source not found.**, the Partial Spearman CC shows absolute values over 0.2 for the "STICK" parameter at the beginning of the transient. This seems to indicate that, even if weak, a monotonic relationship exists between the particle sticking coefficient and the FOM.

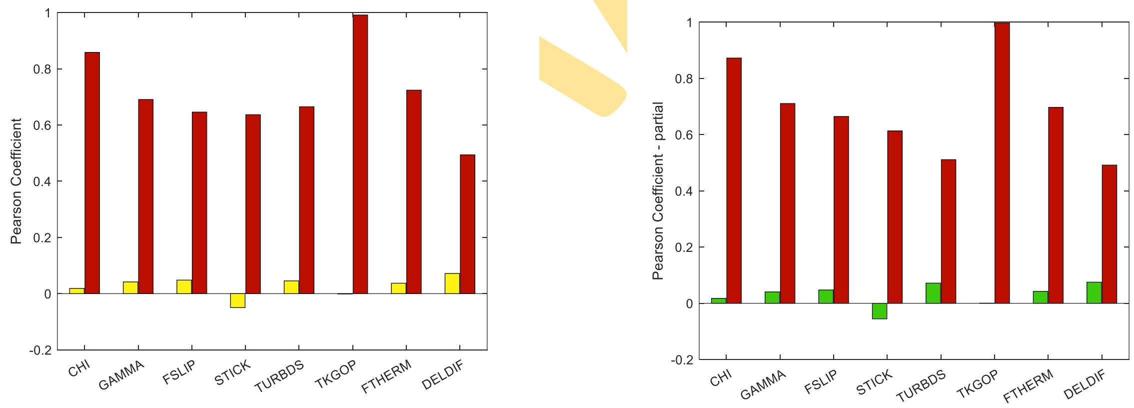

Figure 4: Pearson and Partial Pearson CCs - peak.

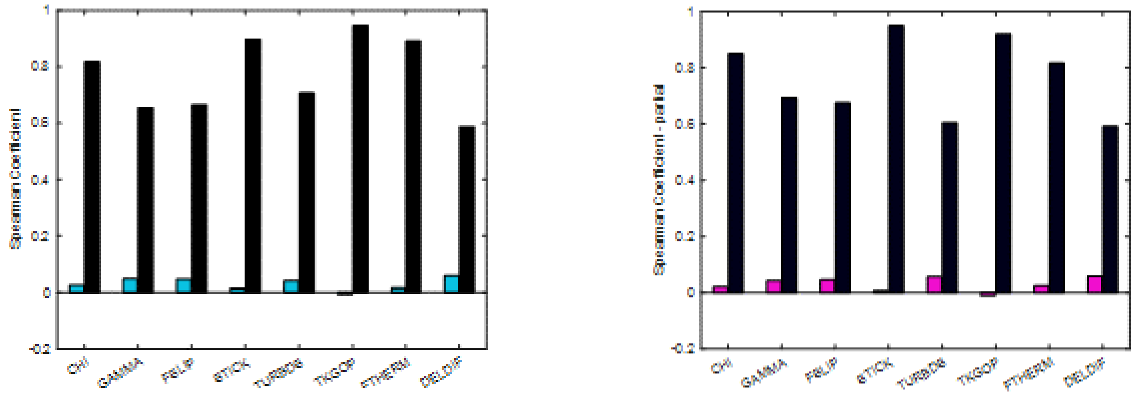

Figure 5: Spearman and Partial Spearman CCs - peak.

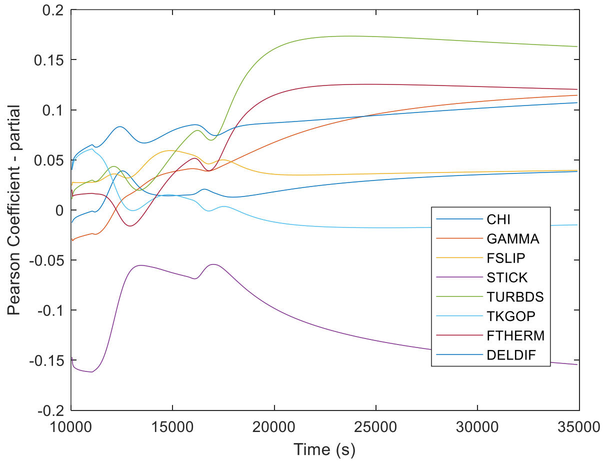

Figure 1: Partial Pearson CC.

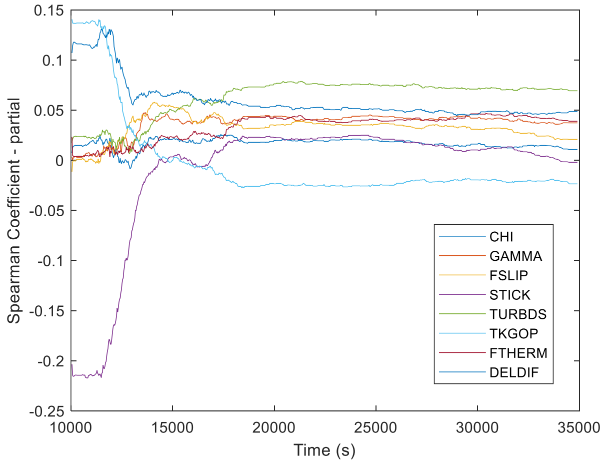

Figure 7: Partial Spearman CC.

CONCLUSIONS

The present paper reports a preliminary UASA of the containment behavior for the PHEBUS FPT1. The study has been conducted on the basis of a standalone model of the containment itself, using the MELCOR 2.2.18019 SA code as the main simulation tool and a series of MATLAB scripts for the UA.

Considering that the correct estimation of a possible radiological source term to the environment is of high relevance to the safety assessment of NPPs, the main focus of the work has been placed on the FOM "mass of aerosol suspended in the containment atmosphere".

The uncertainty investigation has been carried out through the propagation of a limited set of input parameters, all related to aerosol characterization and behavior. The two-sided Wilks formula has been used to calculate the minimum number of runs necessary to achieve a 95%/95% confidence and probability levels on the simulations' results.

The sensitivity analysis has been conducted, as a first approach, by means of CCs, in the attempt to establish the existence of linear and/or monotonic relationships between the selected input parameters and the addressed FOM.

Results show that, as it could be expected, a certain amount of uncertainty exists for what concerns the quantity of aerosol mass suspended in the containment atmosphere. The uncertainty interval varies in time along with the scenario unfolding, and it presents a wide broadening concurrently with the reaching of the peak of aerosol mass in the containment atmosphere, likely due to the complexity of the phenomena involved. Moreover, a tendency to underestimate the maximum value of the aerosol in the containment atmosphere is shown.

As for the sensitivity analysis, no one of the input parameters seems to have a predominant influence when addressing the maximum value of the FOM. In fact, CCs present very low values, and their respective p-values are high. On the other hand, when extending the analysis to the entire calculation time, the Partial Spearman CC shows absolute values over 0.2 for the particle sticking coefficient (STICK) at the beginning of the transient, suggesting the existence of a monotonic relationship, even if weak.

Further analyses have to be performed in order to deeper investigate the influence of a different (and larger) set of parameters. Attention should be also paid to the simultaneous analysis of two or more FOMs (i.e., "aerosol suspended in the containment atmosphere" together with "aerosol deposited in the containment") to have a more thorough uncertainty assessment.

ACKNOWLEDGMENTS

This project has received funding from the Euratom research and training programme 2014-2018 under grant agreement No 847441. The paper reflects only the author's view and the Commission is not responsible for any use that may be made of the information it contains.

REFERENCES

[1] B. Clément and R. Zeyen, "The objectives of the Phébus FP experimental programme and main findings," Ann. Nucl. Energy, vol. 61, pp. 4–10, 2013, doi: 10.1016/J.ANUCENE.2013.03.037.

[2] A. C. Gregoire et al., "PHEBUS FP FT2 Final Report," Saint-Paul-Les-Durance (F), 2008.

[3] P. March and B. Simondi-Teisseire, "Overview of the facility and experiments performed in Phébus FP," Ann. Nucl. Energy, vol. 61, pp. 11–22, 2013, doi: 10.1016/J.ANUCENE.2013.03.040.

[4] D. Jacquemain, S. Bourdon, A. de Braemaeker, and A. Barrachin, "PHEBUS FTP1 Final Report," 2000.

[5] B. Clément and T. Haste, "Comparison Report on International Standard Problem ISP-46 (Phebus FPT1)," 2003.

[6] B. Clément et al., "Thematic network for a Phebus FPT1 international standard problem (THENPHEBISP)," Nucl. Eng. Des., vol. 235, no. 2–4, pp. 347–357, 2005, doi: 10.1016/J.NUCENGDES.2004.08.057.

[7] A. V. Jones et al., "Validation of severe accident codes against Phebus FP for plant applications: status of the PHEBEN2 project," Nucl. Eng. Des., vol. 221, no. 1–3, pp. 225–240, Apr. 2003, doi: 10.1016/S0029-5493(02)00340-0.

[8] J.-H. Park, D.-H. Kim, and H.-D. Kim, "Summary of the Results From the Phebus Fpt-1 Test for a Severe Accident and the Lessons Learned With Melcor," Nucl. Eng. Technol., vol. 38, no. 6, pp. 535–550, 2006.

[9] L. E. Herranz, M. Vela-García, J. Fontanet, and C. L. del Prá, "Experimental interpretation and code validation based on the PHEBUS-FP programme: Lessons learnt from the analysis of the containment scenario of FPT1 and FPT2 tests," Nucl. Eng. Des., vol. 237, no. 23, pp. 2210–2218, Dec. 2007, doi: 10.1016/J.NUCENGDES.2007.03.022.

[10] J. Birchley, "Assessment of the MELCOR Code Against PHEBUS Experiment FPT-1 Performed in the Frame of ISP-46," Proc. Int. Conf. Nucl. Eng., vol. 3, pp. 551–560, Nov. 2008, doi: 10.1115/ICONE12-49267.

[11] J. Wang et al., "Simulation of the PHEBUS FPT-1 experiment using MELCOR and exploration of the primary core degradation mechanism," Ann. Nucl. Energy, vol. 85, pp. 193–204, Nov. 2015, doi: 10.1016/J.ANUCENE.2015.05.015.

[12] T. Haste, F. Payot, and P. D. W. Bottomley, "Transport and deposition in the Phébus FP circuit," Ann. Nucl. Energy, vol. 61, pp. 102–121, Nov. 2013, doi: 10.1016/J.ANUCENE.2012.10.032.

[13] P. Darnowski, M. Włostowski, M. Stępień, and G. Niewiński, "Study of the material release during PHÉBUS FPT-1 bundle phase with MELCOR 2.2," Ann. Nucl. Energy, vol. 148, p. 107700, Dec. 2020, doi: 10.1016/J.ANUCENE.2020.107700.

[14] M. Laurie, P. March, B. Simondi-Teisseire, and F. Payot, "Containment behaviour in Phébus FP," Ann. Nucl. Energy, vol. 60, pp. 15–27, Oct. 2013, doi: 10.1016/J.ANUCENE.2013.03.032.

[15] F. Martín-Fuertes, R. Barbero, J. M. Martín-Valdepeñas, and M. A. Jiménez, "Analysis of source term aspects in the experiment Phebus FPT1 with the MELCOR and CFX codes," Nucl. Eng. Des., vol. 237, no. 5, pp. 509–523, Mar. 2007, doi: 10.1016/J.NUCENGDES.2006.07.006.

[16] A. Kontautas and E. Urbonavičius, "Analysis of aerosol deposition in PHEBUS containment during FPT-1 experiment," Nucl. Eng. Des., vol. 239, pp. 1267–1274, 2009, doi: 10.1016/j.nucengdes.2009.03.012.

[17] G. Gyenes and L. Ammirabile, "Containment analysis on the PHEBUS FPT-0, FPT-1 and FPT-2 experiments," Nucl. Eng. Des., vol. 241, no. 3, pp. 854–864, Mar. 2011, doi: 10.1016/J.NUCENGDES.2010.12.007.

[18] L. E. Herranz et al., "The EC MUSA project on management and uncertainty of severe accidents: Main pillars and status," Energies, vol. 14, no. 15, pp. 1–11, 2021, doi: 10.3390/en14154473.

[19] N. Elsalamouny and T. Kaliatka, "Uncertainty Quantification of the PHEBUS FPT-1 Test Modelling Results," Energies 2021, Vol. 14, Page 7320, vol. 14, no. 21, p. 7320, Nov. 2021, doi: 10.3390/EN14217320.

[20] F. Mascari and al., "First Outcomes From the Phebus Fpt1 Uncertainty Application Done in the Eu-Musa Project," NURETH19, 2022.

[21] F. Mascari et al., "Phebus Fpt1 Uncertainty Application With the Melcor 2.2 Code," NURETH19,2022.

[22] R. Bocanegra and L. E. Herranz, "CIEMAT's outcomes from the PHEBUS-FPT1 uncertainty analysis in the framework of the EU-MUSA project," ERMSAR2022, 2022.

[23] M. Malicki, T. Lind, and J. Kalilainen, "THE PARAMETRIC SENSITIVITY ANALYSIS OF FPT-1 MELCOR 2.2 INPUT DECK AS A PREPARATION FOR UNCERTAINTY QUANTIFICATION STUDY," ERMSAR2022, 2022.

[24] L. L. Humphries et al., "MELCOR Computer Code Manuals, Vol.1: Primer and Users' Guide, Version 2.2.19018," 2021.

[25] L. L. Humphries et al., "MELCOR Computer Code Manuals, Vol. 2: Reference Manual, Version 2.2.18019," 2021.

[26] MATLAB, "R2020b." The MatWorks Inc., 2020.

[27] Wilks S S, “Determination of sample sizes for setting tolerance limits,” Ann. Math. Stat., 1941.

[28] S. S. Wilks, “Statistical Prediction with Special Reference to the Problem of Tolerance Limits,” Ann. Math. Stat., vol. 13, no. 4, pp. 400–409, 1942, doi: 10.1214/aoms/1177731537.

[29] B. Gonfiotti and S. Paci, “Stand-alone containment analysis of the phebus fission products test 1 with the astec and the melcor codes,” J. Nucl. Eng. Radiat. Sci., vol. 4, no. 2, Apr. 2018, doi: 10.1115/1.4038059/442445.

[30] B. Gonfiotti and S. Paci, “Standalone Containment Analysis of Four Phébus Tests with the ASTEC and the MELCOR Codes,” 2019, doi: 10.1155/2019/6021346.

[31] H. Scheurer and B. Clement, “PHEBUS Data Book - FPT1,” 1997.

[32] J. Phillips, A. Notafrancesco, and J. L. Tills, “Application of the MELCOR code to design basis PWR large dry containment analysis.,” Albuquerque, NM, and Livermore, CA (United States), May 2009. doi: 10.2172/959093.

[33] IAEA, “Best Estimate Safety Analysis for Nuclear Power Plants: Uncertainty Evaluation, Safety Reports Series 52,” 2008.

[34] F. D’Auria and A. Petruzzi, “Background and Qualification of Uncertainty Methods,” 2008.

[35] H. Glaeser, “GRS method for uncertainty and sensitivity evaluation of code results and applications,” Sci. Technol. Nucl. Install., vol. 2008, 2008, doi: 10.1155/2008/798901.

[36] N. W. Porter, “Wilks’ formula applied to computational tools: A practical discussion and verification,” Ann. Nucl. Energy, vol. 133, pp. 129–137, 2019, doi: 10.1016/j.anucene.2019.05.012.

[37] M. Salay, D. A. Kalinich, R. O. Gauntt, and T. E. Radel, “Analysis of main steam isolation valve leakage in design basis accidents using MELCOR 1.8.6 and RADTRAD.,” Oct. 2008, doi: 10.2172/1028885.

[38] S. Boslaugh and P. A. Watters, Statistics in a nutshell, vol. 26, no. 1. O’Reilly, 2008.

[39] M. M. Mukaka, “A guide to appropriate use of Correlation coefficient in medical research,” Malawi Med. J., vol. 24, no. 3, p. 69, 2012, Accessed: Nov. 23, 2022. [Online]. Available: /pmc/articles/PMC3576830/.

[40] C. Spearman, “The Proof and Measurement of Association between Two Things,” Am. J. Psychol., vol. 15, no. 1, p. 72, Jan. 1904, doi: 10.2307/1412159.

[41] P. Bruce, A. Bruce, and P. Gedeck, Practical Statistics for Data Scientists (2nd edition). 2020.

[42] A. Wald, “An Extension of Wilks’ Method for Setting Tolerance Limits,” Ann. Math. Stat., vol. 14, no. 1, pp. 45–55, 1943, doi: 10.1214/aoms/1177731491.

[43] MathWorks Inc., “Kernel smoothing function estimate for univariate and bivariate data - MATLAB ksdensity.” https://it.mathworks.com/help/stats/ksdensity.html#btn1_ga-3.